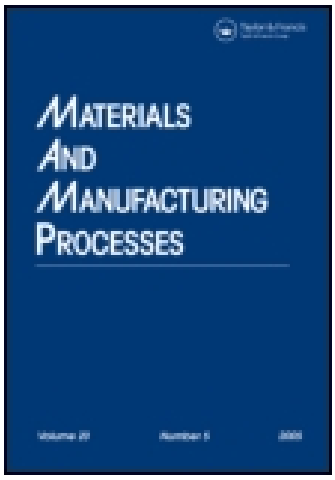

Materials and Manufacturing Processes
Publication details, including instructions for authors and subscription information:
http://www.tandfonline.com/loi/lmmp20

Improvement of Shape-Memory Characteristics and Mechanical Properties of Copper-Zinc-Aluminum Shape-Memory Alloy with Low Aluminum Content by Grain Refinement

V. Sampath [a]
[a] Department of Metallurgical and Materials Engineering , Indian Institute of Technology, Madras , Chennai , India
Published online: 15 Mar 2007.

To cite this article: V. Sampath (2006) Improvement of Shape-Memory Characteristics and Mechanical Properties of Copper-Zinc-Aluminum Shape-Memory Alloy with Low Aluminum Content by Grain Refinement, Materials and Manufacturing Processes, 21:8, 789-795, DOI: 10.1080/10426910600837756

To link to this article: http://dx.doi.org/10.1080/10426910600837756

Materials and Manufacturing Processes, 21: 789–795, 2006

ISSN: 1042-6914 print/1532-2475 online
DOI: 10.1080/10426910600837756

Taylor & Francis
Taylor & Francis Group

Improvement of Shape-Memory Characteristics and Mechanical Properties of Copper–Zinc–Aluminum Shape-Memory Alloy with Low Aluminum Content by Grain Refinement

V. Sampath

Department of Metallurgical and Materials Engineering, Indian Institute of Technology, Madras, Chennai, India

Shape-memory alloys (SMAs) are used as sensors and actuators in most engineering and medical applications and are optimized to exhibit either high stress recovery or high strain recovery. But most binary and ternary Cu-base SMAs are brittle and show low strain recovery due to the coarse grains obtained during solidification. Many new methods, such as powder metallurgy, rapid solidification, multipass rolling and equal-channel angular extrusion, are now being used to produce Cu-base shape-memory alloys with fine grains. However, these methods usually yield the alloys in small quantities despite the fact that each of them has its own advantages and limitations. Casting continues to be the most common and easiest method that helps produce SMAs in large quantities. To overcome the formation of coarse grains during casting, grain-refining additions were made to the liquid alloy. But the extent of grain refining achieved and, in turn, its effect on the shape recovery strain, varies from one study to another. The present work shows that by very small additions of Zr and Ti to a CuZnAl SMA with a low Al content, the shape-recovery strain can be increased to as high as 8%. The alloy also shows higher hardness and ductility after grain refinement.

Keywords Grain refinement; Grain size; Intergranular cracking; Martensite; Mechanical properties; Quenching; Shape-memory effect; Shape recovery; Superelasticity.

Introduction

Shape-memory alloys are used in a wide variety of engineering and medical applications [1–3]. In most of these applications, they function either as sensors or as actuators. The SMAs that are used in sensors and actuators are optimized to exhibit either high stress recovery or high strain recovery. Although Cu–Zn–Al alloys exhibit shape-memory effect, unlike Ni–Ti alloys they are not so widely used since they possess poor mechanical and shape-memory characteristics. This is attributed to the coarse grains obtained as result of solidification of the alloy ingots. Casting is the easiest and most common method that is used to produce the alloys in large quantities. But conventional casting methods by and large yield ingots that abound in solidification-related defects, such as gas porosity, shrinkage porosity, coarse grain, segregation, pipe and inclusion. Coarse grains in particular are undesirable since they impair the mechanical strength, ductility and especially the strain recovery of the shape-memory alloys. In addition, they modify the transformation temperatures of the alloys. The coarse-grained Cu-base SMAs undergo grain growth [4] while reheating of the ingots prior to mechanical working, and also during solution treatment prior to quenching. When the grain size of the Cu-base SMAs is in the millimeter range and the elastic anisotropy is high, the alloys undergo intergranular cracking during quenching or plastic deformation or in service.

Received January 14, 2006; Accepted May 19, 2006

Address correspondence to V. Sampath, Department of Metallurgical and Materials Engineering, Indian Institute of Technology, Madras, Chennai 600 036, India; Fax: 091-044-22574752; E-mail: vsampath@iitm.ac.in

With a view to producing fine-grained Ni–Ti and Cu-base SMAs, many new manufacturing methods, such as chemical reactions in molten salts [5], powder metallurgy/mechanical alloying [6–8], rapid solidification/melt spinning [9], combustion synthesis [10, 11], shock synthesis [12], severe plastic deformation [13] and equal-channel angular extrusion [14], are now being used. But these methods by and large yield alloys in small quantities, though each of these methods has its own advantages and limitations. Casting seems to be the only method that yields the alloys in large quantities. To overcome the formation of coarse grains during casting, grain-refining additions are made to the liquid alloy. This continues to be the most common and easiest method. But the extent of grain refinement achieved and, in turn, its effect on the recovery strain achieved by shape-memory effect varies from one study to another depending on the alloy composition and processing conditions. It is obvious since grain refining brings about concomitant changes in transformation temperatures and shape memory characteristics.

The ternary Cu–Al–Ni SMAs are highly brittle. There are two reasons that are attributed to this behavior: (a) formation of the brittle phase $\gamma_2(Cu_9Al_4)$ and (b) formation of coarse grains during solidification. The brittleness is decreased by the suppression of the formation of γ_2 by adding elements like Mn with low e/a ratios and by using grain-refiners like Zr and B. The high ductility is attributed to the presence of brittle particles that help relieve stress concentrations at grain boundaries [15].

A number of elements, such as Co, Ti, B, Zr, and V are used separately and in varying amounts as grain refiners in Cu–Zn–Al SMAs. The efficacy and the mechanism of grain refinement vary depending upon the alloy composition and the type of grain refining element added. This is because the

particles that are formed strongly depend on the type and the amount of grain refining additions made. The results obtained from these studies [4, 15, 16, 18–22] show that in most cases the strain recovery achieved goes up to 6%. In SMAs, the grain size plays a very significant role in influencing the ductility, mechanical strength, hardness, shape recovery strain and transformation temperatures. Although there is a wealth of information available on the grain refinement of Al, Cu and other alloys, there still is a paucity of published research work pertaining to the grain refinement of Cu-base shape-memory alloys.

The primary objectives of the present work are, therefore, to refine the grain size of Cu–Zn–Al shape-memory alloy chosen and thereby increase its mechanical properties and shape-memory characteristics, especially its strain recovery. The study shows that considerable improvements in the shape memory and other properties of the alloy are achieved. The improvements achieved are correlated to the microstructure.

Experimental procedure

A Cu–Zn–Al alloy with 30.36% by weight of Zn and 2.19% by weight of Al was prepared using high purity (99.9 wt.%) Cu, Al, and Zn ingots. Grain refiners in the form of Zr, Ti, and B, to the extent of 0.2 wt.% each, were added but separately to the alloy during melting. The required quantities of Cu and Al, together with the grain refiners, were taken in a graphite crucible, and the crucible was then placed inside a resistance-heated muffle furnace. The melting was carried out under a protective atmosphere of argon. The loss of Zn by evaporation from Cu–Zn–Al alloys is a problem that is to be overcome during melting of Cu–Zn–Al SMAs. The Zn in appropriate quantity was, therefore, added to the melt towards the end so as to compensate for its excessive evaporation. Cupric oxide was also used as a flux to protect the molten metal from undergoing oxidation. The molten alloy was poured into cast iron molds and allowed to solidify. The alloy ingots so obtained were given a homogenization treatment at 1073 K for 7.2 ks. The ingots were then quenched into water at room temperature so as to obtain a completely martensitic structure. The samples for microstructural examination, X-ray diffraction and differential scanning calorimetry studies were then machined out from the cast ingots. The alloy was rolled at 1073 K to obtain sheets of 0.001 m thickness. The samples for the bend and tension tests were machined out from the rolled sheets. The phase and crystal structure analyses were carried out by XRD using CuKα radiation. The microstructure was studied by optical microscopy. A 10% potassium dichromate solution was used as the etchant. The characteristic transformation temperatures were determined by a Netzch 204 differential scanning calorimeter using the alloy filings at a scanning rate of 5 K/min. Hardness tests were also carried out on the samples. Figure 1 is a flow chart that illustrates the different steps involved in the preparation, processing and characterization of the alloy.

Tension tests were carried out on sheet samples measuring 0.1 m × 0.005 m × 0.001 m in size using a specially designed test setup, shown in Fig. 2. In this setup, one end of the sample was permanently fixed and the free end

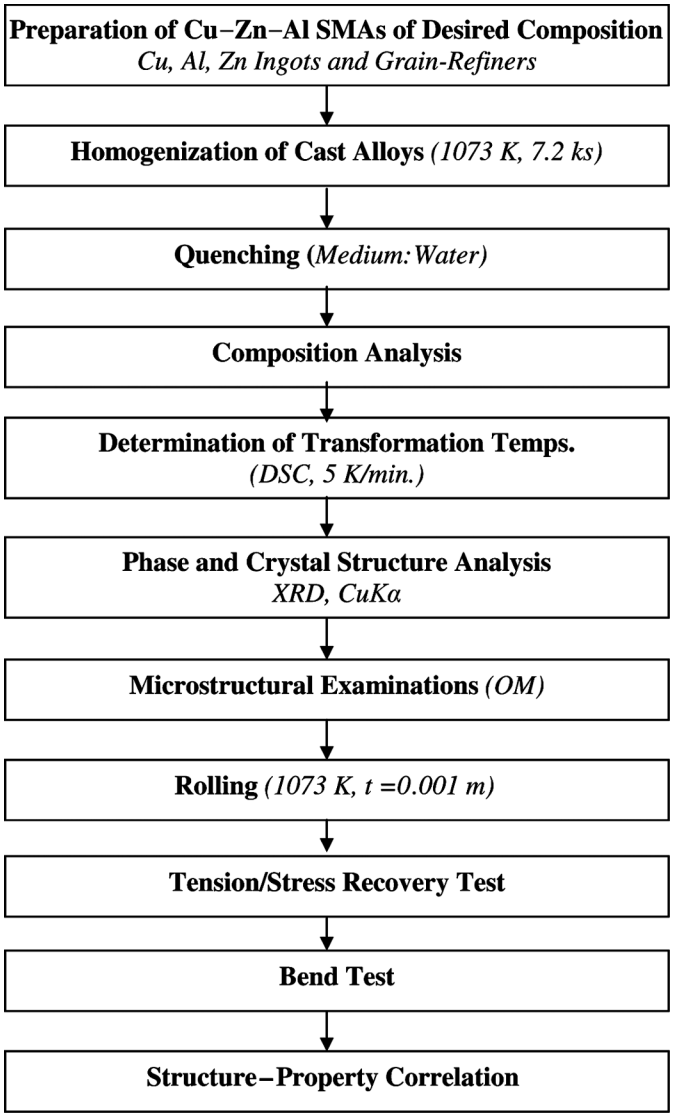

Figure 1.—Flowchart giving details of preparation, processing and characterization of Cu–Zn–Al shape memory alloys.

was used to suspend a load cell by a string of wire via a pulley. The sample was heated by passing an electric current through a heating coil made of Kanthal wound around it. The temperature of the sample was measured using a Pt–Pt–16Rh thermocouple. The stress and strain were measured as a function of temperature. The strain recovered was measured using the load cell at every 5 K interval. The samples were prestrained up to 8–9% in a universal testing machine (UTM) by applying a maximum load of 88 N (90 kg). The deformation characteristics of the Cu–Zn–Al shape-memory alloys were determined by plotting the stress–strain curves based on the values obtained from the test. After prestraining, the strain recovery of the samples was estimated in terms of strain and temperature.

Bend tests were carried out on sheet samples made from the hot-rolled sheets. A schematic diagram of the bend test is given in Fig. 3. The samples were wrapped around a steel rod/mandrel of known diameter. The prestrain given to the

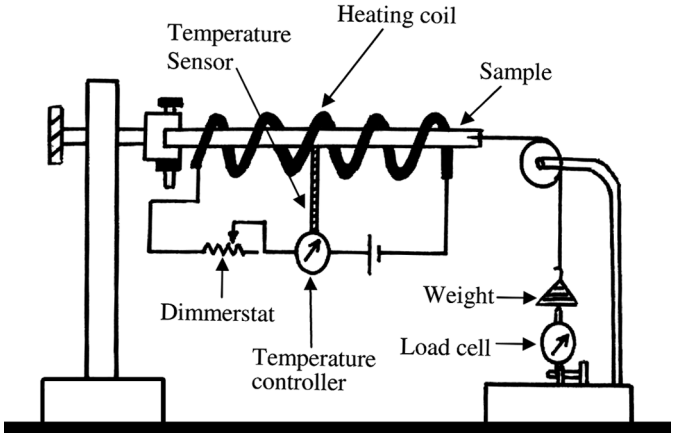

FIGURE 2.—Schematic diagram of experimental setup used for measurement of stress, strain and temperature of Cu–Zn–Al alloys with and without grain-refining additions.

sample was determined using the equation $\varepsilon = t/d$, where ε is the strain, t the thickness and d the diameter of the sample.

RESULTS AND DISCUSSION

The grain-refining elements usually form hard and insoluble particles during solidification. These are classified into three types [16] depending on their influence on the grain refinement of Cu-base SMAs: (a) those that do not cause any grain refinement (e.g., Co), (b) those that bring about minor grain refinement (e.g., Ti), and (c) those that cause marked grain refinement (e.g., B).

Figure 4 shows the micrograph of base Cu–Zn–Al alloy without grain-refining additions viewed at a lower magnification showing the occurrence of intergranular cracking. This is an equilibrium microstructure obtained by simply solidifying the liquid alloy from its pouring temperature. The interpretations of the microstructure have been done based on the composition, phase diagram and what has been already reported in the literature. The

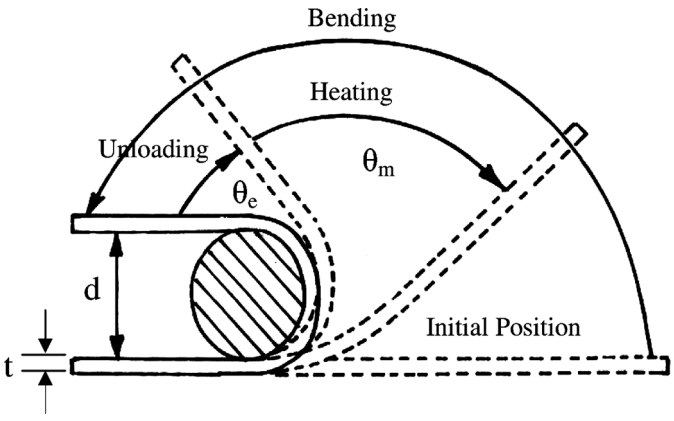

FIGURE 3.—Schematic diagram for bend tests carried out on sheet samples of Cu–Zn–Al shape-memory alloys showing strain recovery by superelastic effect (θ_e) and shape-memory effect (θ_m).

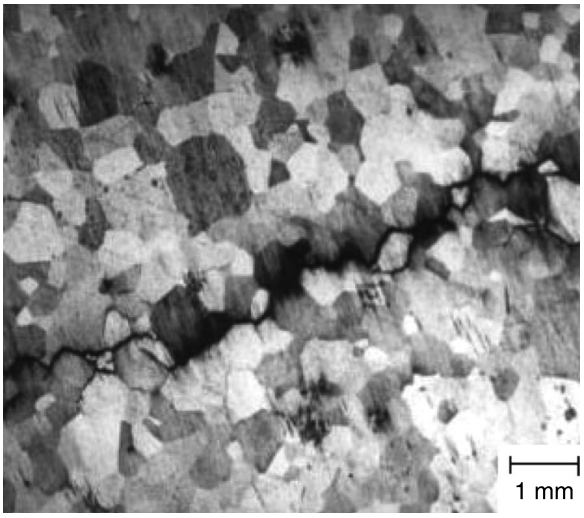

FIGURE 4.—Micrograph of base Cu–Zn–Al alloy without grain-refining additions viewed at a lower magnification showing the occurrence of intergranular cracking. This is an equilibrium structure obtained by simply solidifying the liquid alloy.

micrograph of the parent phase (β) in the Cu–Zn–Al alloy without any grain-refining addition is shown in Fig. 5. The entire microstructure consists of the β phase. This phase crystallizes in a specific morphology as is shown in the micrograph. This phase is obtained when the alloy has a specific composition, i.e., falling within the limits of shape-memory composition. The microstructural examination of the base alloy reveals the presence of coarse grains with an average diameter of 0.0015 m in the as-cast and quenched condition, as is shown in Fig. 6.

The figure shows the microstructure of Cu–Zn–Al alloy without any grain-refining additions, showing coarse grains with twins within the martensitic plates. A, B, C, and D refer to the variants of martensite with a self-accommodating

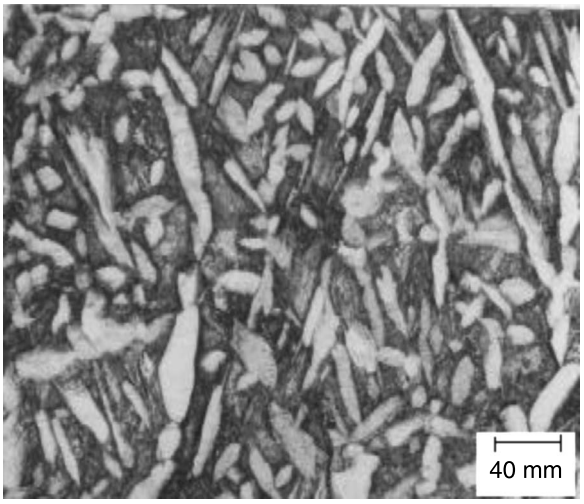

FIGURE 5.—Microstructure of Cu–Zn–Al alloy showing parent phase (β) crystallizing in elongated and irregular morphology.

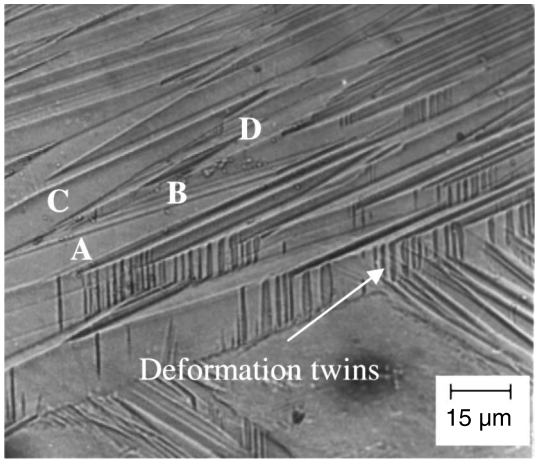

FIGURE 6.—Microstructure of Cu–Zn–Al alloy without any grain-refining additions showing coarse grains with twins within the martensitic plates. A, B, C, and D refer to the variants of martensite with a self-accommodating morphology.

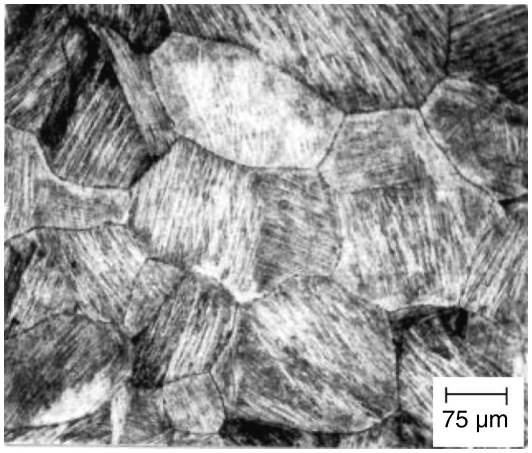

FIGURE 8.—Microstructure of Cu–Zn–Al alloy with Zr addition showing fine grains. Martensitic plates with different orientations can be seen within each of the grains.

morphology. The X-ray diffraction (XRD profile of the alloy) without any grain-refining addition in the quenched condition, shown in Fig. 7, confirms the formation of 18R martensite. The crystal structure of the martensite formed was found to be rhombohedral, which structure is favorable for shape-memory effect. The grain size of the alloy subjected to refinement by adding 0.2 wt.% of Zr was found to be 200 μm, while that with 0.2 wt.% of Ti was found to be 500 μm (Figs. 8 and 9). The microstructure of the alloy with B addition does not show any martensitic structure (Fig. 10) and instead shows a large amount of bulky precipitates that retard the martensitic transformation.

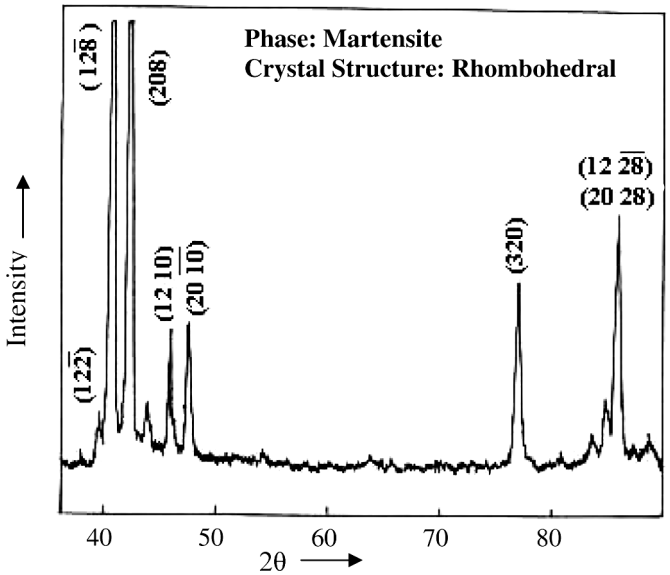

FIGURE 7.—XRD profile of Cu–Zn–Al alloy without any grain-refining additions showing peaks and planes corresponding to martensite with a self-accommodating morphology.

The bulky precipitate particles are probably Al-rich boride particles, as reported in the literature [22]. The characteristic transformation temperatures of the base alloy determined from differential scanning calorimetry (DSC) measurements are indicated in Fig. 11 that is obtained by plotting the results obtained by cooling the alloy. The base alloy has its M_s around 313 K, and its M_f around 305 K.

The most common grain-refining elements [17] and the amount in which they are added to Cu-base SMAs are: Zr = 0.4–1.2 wt.%; Co = 0.4–0.8 wt.%; Ti = 0.5–1.0 wt.%; B = 0.2–0.4 wt.%. These elements reduce the grain diameter to about 100 μm. In an earlier work by Lee and Wayman [18], when Zr was added to Cu–Zn–Al alloys in the range of 0.3–1.3 wt.%, the grain size obtained was <50 μm. On the other hand, when Ti was added in the range of 0.2–0.8 wt.%, the grain diameter obtained was in the range of 50–500 μm. Morawiec et al. [19] used Ti and

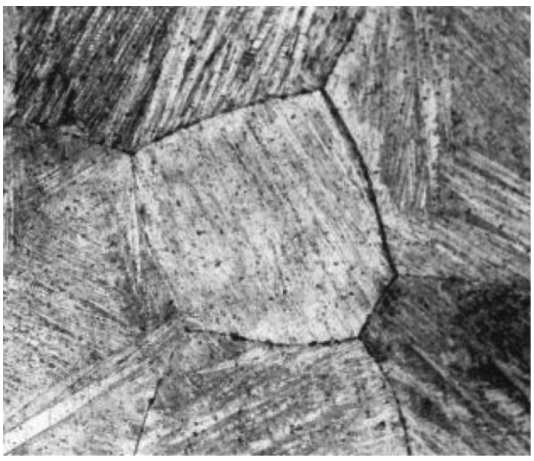

FIGURE 9.—Microstructure of Cu–Zn–Al alloy with Ti addition showing fine grains. Somewhat finer martensitic plates with different orientations can be seen within each of the grains. The orientation changes as the plates approach the grain boundaries.

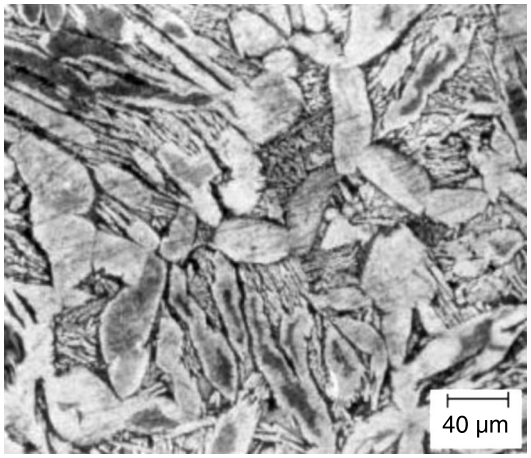

FIGURE 10.—Microstructure of Cu–Zn–Al alloy with B addition showing a region that is rich in bulky precipitate particles with elongated and irregular shapes probably of aluminum-rich boride as reported in the literature [22].

B together as grain-refining elements in Cu–Zn–Al alloys and brought down the grain size to 100 μm, causing thereby a decrease in the grain size by ten times. Elst et al. [16] also used Ti and B and obtained grain sizes in the range of 50–100 μm. Lee and Wayman [18] used a higher amount, i.e., 1.2 wt.%, of Zr, and were able to reduce the grain size to 30 μm.

The grain-refining elements have very low solubilities in Cu-based SMAs. The refinement is, therefore, largely due to the formation of small insoluble particles that either aid in nucleation of new grains or inhibit the growth of existing grains [16]. Part of Ti and B used together is utilized in the formation of TiB_2 particles and the remaining goes into solution in the β-matrix. The TiB_2 particles create stress fields around them and prevent/obstruct the movement of the martensite plates during deformation and shape recovery. Elst et al. [16, 20, 21] and Morris [22] found that the addition of 0.4 wt.% of Co did not bring about any grain refinement at all, while that of 0.5–1.0 wt.% of Ti resulted in a slight reduction in the grain size (due to the formation of Ti-rich particles). They also found that B addition in the range of 0.04–0.2 wt.% brought about considerable reduction in grain size due to the formation of Al-rich boride particles. Grain refining was achieved by the formation of insoluble particles that either aid in the nucleation of grains or retard their growth. The probable reason for the absence of martensite in boron-added samples is the formation of intermetallics based on B that deplete the matrix of alloying elements. Part of the boron added also goes into solution in the β-matrix. These two processes affect the transformation temperatures, especially Ms, and decrease them to below room temperature. This was why martensite could not be obtained in the alloy with B addition.

TABLE 1.—Results of bend tests conducted on sheet samples of base- and grain-refined Cu–Zn–Al alloys.

Material	Superelastic strain	Shape-memory strain
Cu–Zn–Al	0.012	0.064
Cu–Zn–Al + 0.2 wt% Zr	0.008	0.082
Cu–Zn–Al + 0.2 wt% Ti	0.016	0.080

The bend test is useful in determining the extent of strain recovery of the shape-memory alloy with and without any grain-refining additions. The initial prestrain given to the sheet sample was 0.09. This value was arrived at by substituting for d (=0.011 m) and t (=0.001 m) in the equation $\varepsilon = t/d$. After prestraining, the sample was

TABLE 2.—Hardness values of base- and grain-refined CuZnAl alloys.

Material	Hardness number (VHN)
Cu–Zn–Al	135
Cu–Zn–Al + 0.2 wt.% Zr	160
Cu–Zn–Al + 0.2 wt.% Ti	195

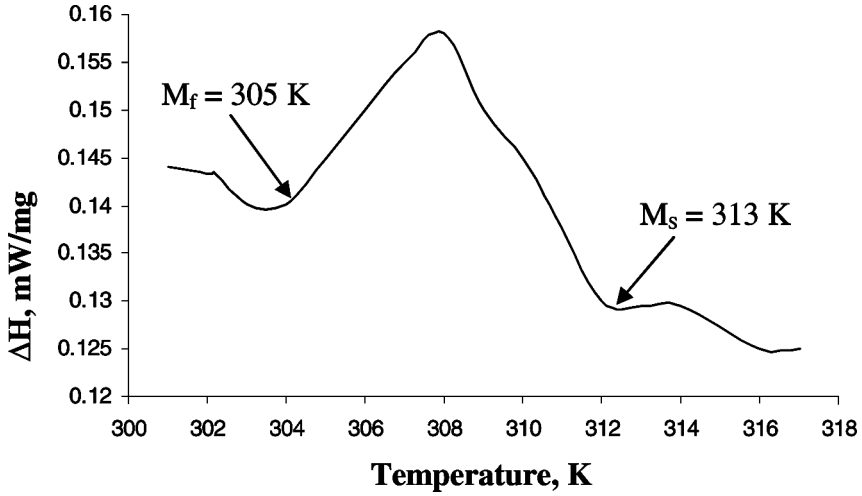

FIGURE 11.—DSC plot for base Cu–Zn–Al alloy showing M_s and M_f temperatures.

heated to about 373 K to cause its reversion to its original/high temperature phase and, in the process, recover its original/initial shape and dimensions. The strain recovery caused by superelasticity and shape-memory effect, respectively, can be calculated by using the relationships: $f_{SE} = \theta_e/180$ and $f_{SME} = \theta_m/(180 - \theta_e)$, where f_{SE} is the fraction of strain recovery due to superelasticity and f_{SME} is that due to shape-memory effect. The results of the bend tests carried out on the sheet samples of the shape memory alloys are given in Table 1. The grain-refined alloys exhibit a much larger strain. This clearly shows the increase in the ductility of the material brought about by grain refinement. Zr addition in particular is most effective. The results indicate that the zirconium-added alloy shows the highest strain recovery, followed by Ti-added and base alloys. The number of self-accommodating variants within a grain increases as the grain size decreases.

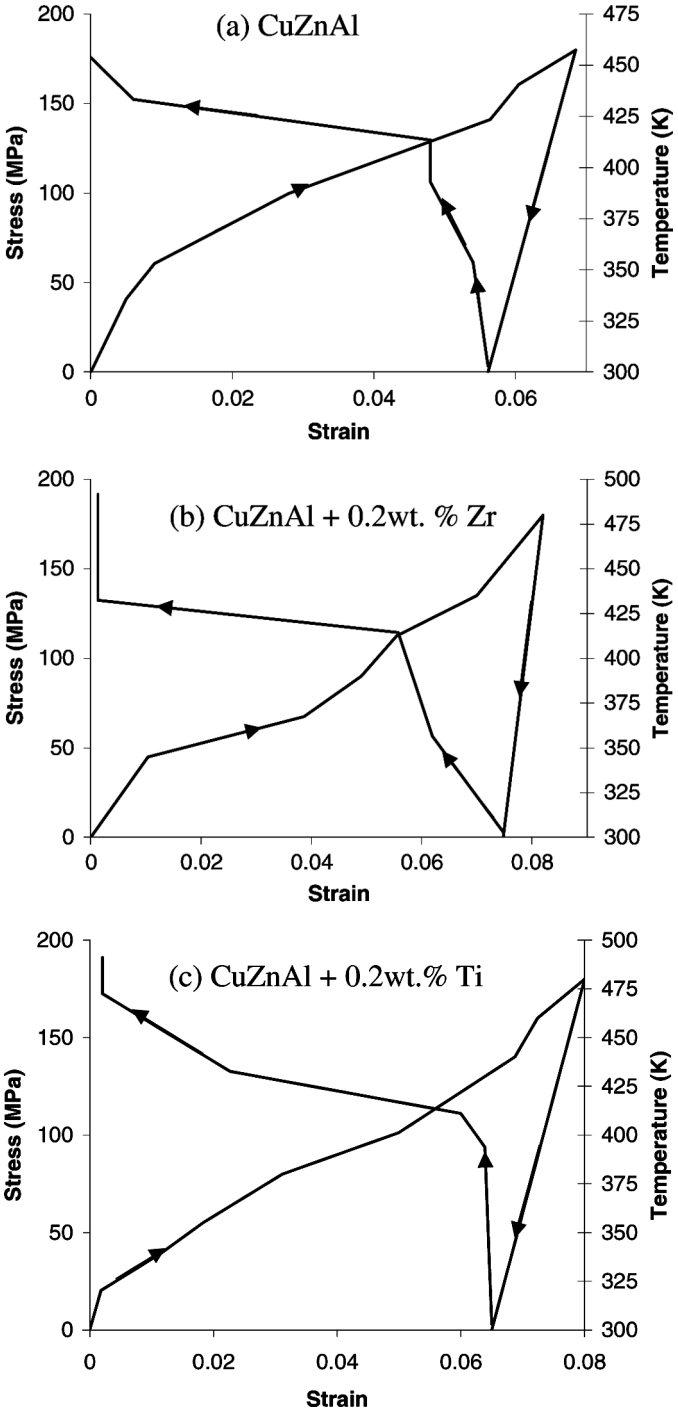

FIGURE 12.—Stress–strain–temperature plots for (a) base-, (b) Zr-added and (c) Ti-added Cu–Zn–Al alloys showing strain recovery by shape memory effect (heating) and superelastic effect (unloading).

The results of the hardness tests are given in Table 2. The alloys that were grain refined with Zr and Ti show higher hardness compared with the base alloy. The increase in hardness is again attributed to the finer grains obtained in Zr- and Ti-added alloys. The results of the tension tests are carried out on the base- and grain-refined alloys are plotted in the form of stress–strain and strain–temperature diagrams in Fig. 12. The results obtained agree well with those obtained from the bend tests. The alloy with Zr addition shows higher strain recovery. The stress–strain–temperature relationships show that plastic deformation starts around 80 MPa. An initial prestrain of 0.09 corresponding to the stress level of 180 MPa was given. The base alloy recovered a strain of about 0.068, out of which 0.012 was the superelastic component. But the Zr- and Ti-added alloys recovered a strain of 0.082 and 0.080, respectively. The increase in strain recovery is attributed to the fact that in the grain-refined alloys the number of variants is large, resulting in a large number of variants responding to the load. Those variants that are favorably oriented coalesce and grow at the expense of the others. Due to space constraints the micrographs depicting the movement of the martensitic variants with applied load are not presented in this paper. The alloy with boron was not tested since it did not exhibit martensitic transformation due to the formation of bulky precipitate particles that prevented the formation of martensitic plates.

CONCLUSIONS

1. The addition of 0.2 wt.% each of Zr and Ti, separately, to the base alloy results in considerable reduction in the grain size, from 1500 μm to 200 μm, giving rise to more than 85% reduction.
2. The grain size reduction is attributed to the suppression of grain growth during casting and subsequent beta solution treatment by the hard particles formed due to the grain-refining additions.
3. The alloy with Zr addition shows higher ductility and shape-memory strain compared with that with Ti addition.
4. Grain-refining leads to an increase in the shape-memory strain (8%) compared with that for the base alloy and other Cu-base shape-memory alloys reported.
5. Grain refinement results in higher hardness of the SMAs.

REFERENCES

1. Van Humbeeck, J. Non-medical applications of shape memory alloys. Mat. Sci. Eng. A **1999**, *273–275*, 134–148.
2. Morgan, N.B. Medical shape memory alloy applications – the market and its products. Mater. Sci. Eng. A **2004**, *378*, 16–23.

3. Duerig, T.W.; Pelton, A.; Stockel, D. An overview of nitinol medical applications. Mat. Sci. Eng. A **1999**, *273–275*, 149–160.
4. Elst, R.; Van Humbeeck, J.; Delaey, L. Grain growth in beta-copper alloys. Z. Metallkd. **1985**, *76*, 704–708.
5. Zhao, J.; Cui, L.; Gao, W.; Zheng, Y. Synthesis of Ni–Ti particles by chemical reaction in molten salts. Intermetallics **2005**, *13*, 301–303.
6. Zhang, S.; Lu, L.; Lai, M.O. Cu-based shape memory powder preparation using the mechanical alloying technique. Mat. Sci. Eng. A **1993**, *171*, 257–262.
7. Tang, S.M.; Chung, C.Y; Liu, W.G. Preparation of Cu–Al–Ni shape memory alloys by mechanical alloying and powder metallurgy method. J. Mater. Process. Tech. **1997**, *63*, 307–312.
8. Maziarz, W.; Dutkiewicz, J.; Van Humbeeck, J.; Czeppe, T. Mechanically alloyed and hot pressed Ni-49.7 Ti alloy showing martensitic transformation. Mat. Sci. Eng. A **2004**, *375–377*, 844–848.
9. Eucken, S.; Donner, P.; Hornbogen, E. On improvement in the mechanical properties of rapidly solidified shape memeory alloys. Mat. Sci. Eng. **1988**, *98*, 469–474.
10. Chu, C.L.; Chung, C.Y.; Lin, P.H. Phase transformation behaviors in Ni-rich Ni-Ti shape memory alloy fabricated by combustion synthesis. Mat. Sci. Eng. A **2005**, *392*, 106–111.
11. Li, B.Y.; Rong, L.J.; Li, Y.Y.; Gjunter, V.E. Synthesis of porous Ni–Ti shape memory alloys by self-propagating high temperature synthesis: reaction mechanism and anisotropy in porous structure. Acta Mater. **2000**, *48*, 3895–3904.
12. Xu, X.; Thadhani, N. Shock synthesis and characterization of nanostructured NITINOL alloy. Mat. Sci. Eng. A **2004**, *384*, 194–201.
13. Pushin, V.G.; Stolyarov, V.V.; Valiev, R.Z.; Kourov, N.I.; Kuranova, N.N.; Prokofiev, E.A.; Yurchenko, L.I. Features of structure and phase transformations in shape memory TiNi-based alloys after severe plastic deformation. Ann. de Chimie Sci. des Matér. **2002**, *27*, 77–88.
14. Li, Z.; Cheng, X.; ShangGuan, Q. Effect of heat treatment and ECAE process on transformation behaviors of Ni–Ti shape memory alloy. Materials Lett. **2005**, *59*, 705–709.
15. Morris, M.A. Influence of boron additions on ductility and microstructure of shape memory Cu–Al–Ni alloys. Scripta Met. Mater. **1991**, *25*, 2541–2546.
16. Elst, R.; Van Humbeeck, J.; Meeus, M.; Delaey, L. Grain refinement during solidification of β-Cu based alloys. Z. Metallkd. **1986**, *77*, 421–424.
17. Van Humbeeck, J.; Stalmans, R. Shape memory alloys, types and functionalities. In *Encyclopedia of Smart Materials*; Mel Schwarz, Ed.; John Wiley & Sons: New York, USA, 2002; pp. 951–964.
18. Lee, J.S.; Wayman, C.M. Grain refinement of Cu–Zn–Al shape memory alloys. Metallography **1986**, *19*, 401–419.
19. Morawiec, H.; Bojarski, Z.; Lelatko, J.; Joszt, K. Grain refinement of Cu–Zn–Al shape memory alloys. Z. Metallkd. **1990**, *81*, 419–423.
20. Elst, R.; Van Humbeeck, J.; Delaey, L. Grain refinement of Cu–Zn–Al and Cu–Al–Ni by Ti addition. Mater. Sci. Technol. **1988**, *4*, 644–648.
21. Elst, R.; Van Humbeeck, J.; Delaey, L. Evaluation of grain growth criteria in particle-containing materials. Acta Met. **1988**, *36*, 1723–1729.
22. Morris, M.A. High temperature properties of ductile Cu–Al–Ni shape memory alloys with boron additions. Acta Metall. Mater. **1992**, *40*, 1573–1586.